Flow~Induced Vibration

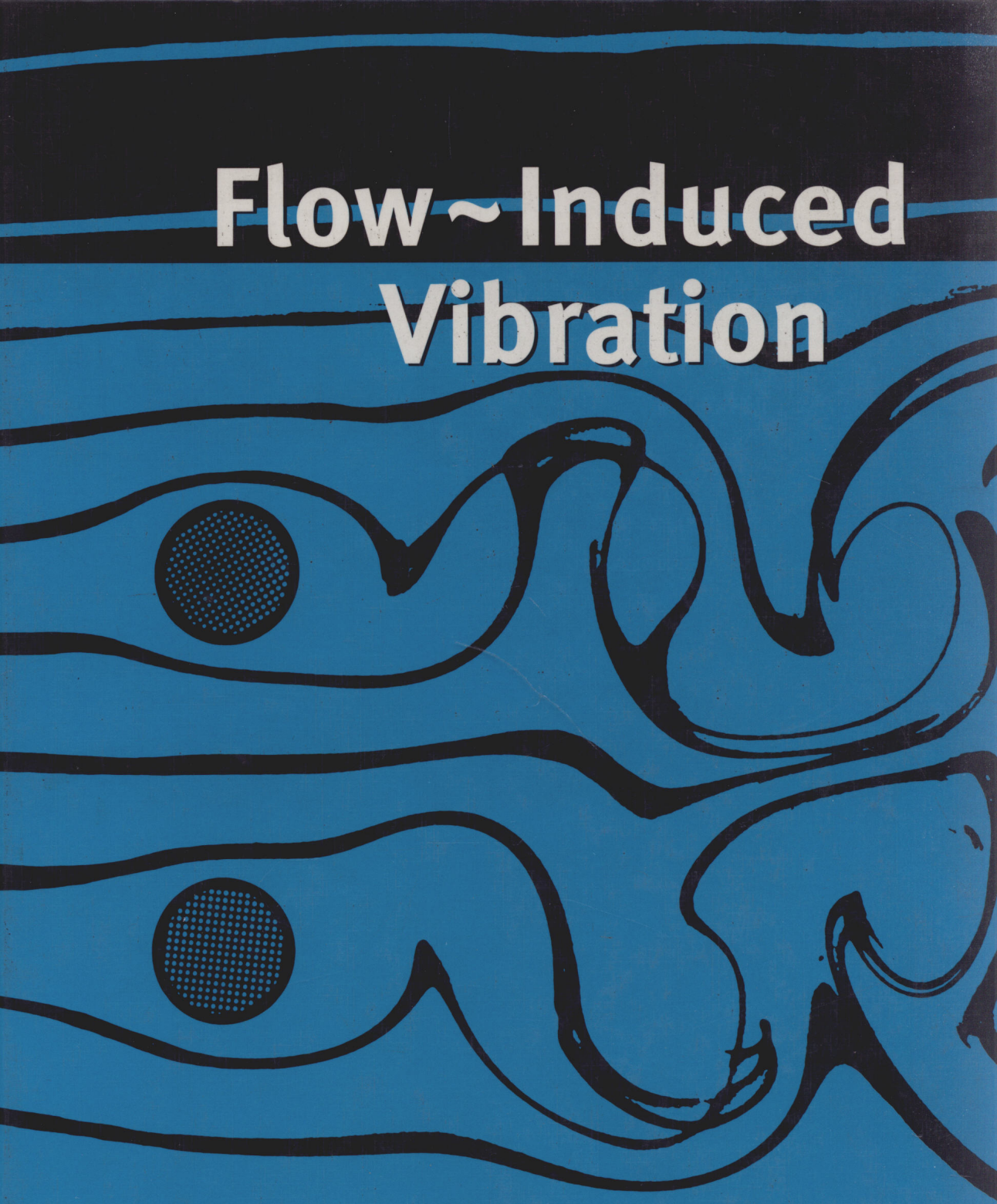

Edited by P.W. Bearman

Photo cover: courtesy of J.O'Leary

The texts of the various papers in this volume were set individually by typists under the supervision of either each of the authors concerned or the editor.

Published by
A.A.Balkema, P.O.Box 1675, 3000 BR Rotterdam, Netherlands (Fax: +31.10.413.5947)
A.A.Balkema Publishers, Old Post Road, Brookfield, VT 05036, USA (Fax: +1.802.276.3837)

ISBN 90 5410 547 X

Printed in the Netherlands

Flow-Induced Vibration, Bearman (ed.) © 1995 Balkema, Rotterdam. ISBN 90 5410 547 X

Preface

The first International Conference on Flow-Induced Vibration was held at Keswick in 1973 and the majority of the papers at this, and the next few conferences in the series, were aimed primarily at the needs of the nuclear industry. Following the trend set at the last two meetings, the papers presented at the sixth conference address a much larger range of application areas. The vibration of structures caused by dynamic fluid loading is a problem which is being experienced in a wide range of industries from civil engineering, marine structures and transportation to power generation and chemical processes. The Organising Committee set as its aim to bring together those working on the mechanisms and causes of vibration with those in industry who are faced with either avoiding the problem through good design or finding a solution to a specific problem in working plant or an existing structure.

Over the years a great deal of research has been carried out into the problem of flow-induced vibration of heat exchanger tube arrays to single phase cross and axial flow, and the understanding and prediction of this type of vibration remains a very active area of investigation. Equally important is the understanding of the vibration mechanisms of tubes in two phase flows. Regular vortex shedding is a well known cause of flow-induced vibration of bluff cylinders yet aspects of this problem remain poorly understood. A significant new development is the increasing application of computational fluid dynamics to the calculation of flow around oscillating cylinders and hence to the prediction of vibration levels. A number of papers in these areas are brought together in the proceedings. Other topics covered include the vibration of hydraulic gates, the interaction between a fluid and a rotating shaft, the vibration of offshore structures, their components and underwater cables due to currents and waves, the vibration of valves and piping systems and wind-induced vibration of buildings and structures. Advances in fluid/structure interaction theory are presented together with papers in the interesting area of flow-induced vibration control.

All the members of the Organising Committee and the Scientific Committee listed below are thanked for their valuable advice and their assistance in bringing these papers together. An acknowledgement is also due to Roslee Fairhurst of Imperial College for her helpful and efficient administrative support. Last but not least, the authors are thanked for providing such an interesting set of papers.

Peter Bearman
Imperial College, London
January 1995

Flow-Induced Vibration, Bearman (ed.) © 1995 Balkema, Rotterdam. ISBN 90 5410 547 X

Organisation

Scientific Committee

P.W. Bearman (Chairman)*, Imperial College, London, UK
B.L. Clarkson*, University College Swansea, Swansea, UK
H. Försching, DLR, Göttingen, Germany
H.G.D. Goyder*, AEA Technology, Harwell, UK
J.M.R. Graham*, Imperial College, London, UK
K. Kamemoto, Yokohama National University, Yokohama, Japan
Y. Nakamura, Kyushu University, Kasuga, Japan
M.P. Paidoussis, McGill University, Montreal, Canada
D. Rockwell, Lehigh University, Bethlehem, USA
D.S. Weaver, McMaster University, Hamilton, Canada
L.R. Wootton*, City University, London, UK
S. Ziada, Sulzer Innotec AG, Winterhur, Switzerland

*Member of Organising Committee

Flow-Induced Vibration, Bearman (ed.) © 1995 Balkema, Rotterdam. ISBN 90 5410 547 X

Table of contents

Vortex-induced vibration

Flow-Induced Vibration, Bearman (ed.) © 1995 Balkema, Rotterdam. ISBN 90 5410 547 X

Vortex shedding lock-on in a circular cylinder wake

Owen M. Griffin
Naval Research Laboratory, Washington, D.C., USA
Mary S. Hall
Science Applications International Corporation, McLean, Va., USA

ABSTRACT: The vortex shedding lock-on which results from crossflow cylinder oscillations has been studied extensively over many years. Among the recent experiments are those of Cheng and Moretti (1991). The results of their experiments at Reynolds numbers of 1500 and 1650 are in good agreement with the earlier experiments of Koopmann (1967) at the lower Reynolds number of Re=200. Cheng and Moretti showed that the upper boundary of the *primary or fundamental* lock-on amplitudes is self-limiting over the range of frequencies in which the phenomenon occurs. The character of the vortex shedding undergoes some important changes within this range of amplitudes and frequencies, as shown by flow visualization at Re=200. Visualization photographs of the near-wake shedding structure from NRL are in very good agreement with the recent computations of Meneghini and Bearman (1993) at this same Reynolds number of 200. Many of the same lock-on characteristics have been observed when the cylinder is vibrated in-line with the flow or the incident flow has a periodic component superimposed on it (Hall and Griffin 1993). These cases also will be discussed in the paper. The importance of the near-wake vortex formation processes to the overall shedding and lock-on also is discussed in terms of recent work.

1 INTRODUCTION

Vortex streets are formed in the wakes of cylindrical bluff bodies over a wide range of Reynolds numbers, from approximately 50 to 10^6 and even higher. The physics of vortex street formation and the near-wake flow has been the focal point of interest for many experimental studies. A recent example is the investigation of bluff body vortex formation and vorticity generation by Green and Gerrard (1993), which advances the earlier work of Gerrard (1966, 1978) and of Bloor and Gerrard (1966). The relation between the vortex formation and vorticity generation is discussed further by Griffin (1995). Recent advances in stability theory have shown that the vortex formation region is one of global absolute instability (Rockwell 1990; Schumm, Berger and Monkewitz 1994). This recent work by several investigators has fundamentally changed our perception of the near-wake physics.

One reason for this continued interest is the importance of knowing how the mean and fluctuating fluid forces are generated on the body due to the vortex shedding. Another is the perceived influence or 'footprint' of the near-wake flow in the eventual evolution of the overall middle- and far-wake flow

When a bluff cylinder in a flow is excited by fields (Cimbala et al. 1988). resonant oscillations, the cylinder and its shed vortices have the same frequency near one of the body'scharacteristic frequencies (Koopmann 1967, Sarpkaya 1979, Bearman 1984, Griffin and Hall 1991). This coincidence or resonance of the shedding and oscillation frequencies is commonly termed lock-on, and such a state emerges when the body is externally oscillated in various orientations relative to the incident flow over the appropriate range of imposed frequencies and amplitudes (Koopmann, 1967; Griffin and Ramberg, 1974, 1976; Ongoren and Rockwell 1988; Nuzzi et al. 1992). Self-excited oscillations and lock-on occur when the body is tuned and free to oscillate.

Vortex resonance or lock-on is observed experimentally when the incident mean flow has a sufficiently large periodic component superimposed upon it (Griffin and Hall 1991). The cylinder remains

stationary in the flow, but the vortex lock-on or resonance produced by inflow pertur-bation modifies the character of the near-wake flow. This form of perturbation is equivalent to the in-line oscillations when the acoustic wavelength is long compared to the cylinder diameter. Vortex resonance or lock-on due to inflow perturbations has been studied computationally by Hall and Griffin (1993), and experimentally by Barbi, Favier, Maresca and Telionis (1986).

Improvements in both computing power and numerical simulation capabilities now complement the many experiments already performed and allow the bluff body flow field to be computed to very high resolutions in both two and three dimensions. Some recent examples are given by the work of Karniadakis and Triantafyllou (1989, 1992), Hall and Griffin (1993), and Meneghini and Bearman (1993).

Vortex lock-on and resonance phenomena have numerous practical engineering applications in addition to their fundamental physical importance. The practical aspects of the problem are discussed in an article by Moretti (1993). Applications abound in offshore exploration and drilling, naval and marine hydrodynamics, and underwater acoustics. Other areas of engineering practice where these phenomena play important roles are civil and wind engineering, nuclear and conventional power generation, and electric power transmission.

2 BLUFF BODY VORTEX FORMATION

The flow in the vortex formation region of a bluff body is important to the overall development of the near-wake flow, and to the ensuing physical evolution of the wake. This is the region of the flow where the vortex shedding is initiated at all Reynolds numbers. Visualization of the vortex formation region for a circular cylinder is shown here in Fig. 2(a) where the vortex formation region length is measured from the center of the cylinder. This photograph of the wake at Re=200 illustrates clearly the phenomenological model originally proposed by Gerrard (1966). The clarity and two-dimensionality of the vortex formation region are increased by the stabilizing crossflow oscillations of the cylinder.

According to Gerrard, the growing vortex is fed by circulation from the separated shear layer until it becomes strong enough to roll up and draw the opposing shear layer across the wake. This vorticity of opposing sign cuts off further circulation to the growing vortex, which then is shed and moves away downstream. There is a delicate balance between the vorticity which is 'a' entrained into the growing vortex, 'b' entrained into the separated shear layer, and 'c' cancelled in the next half of the shedding cycle. The entrained vorticity 'b' plays a key role in Gerrard's model. This is the high-Re mechanism discussed by Green and Gerrard (1993).

The high and low Reynolds number ranges vary somewhat as they are defined in the literature, for example, by Roshko (1954, 1955), Gerrard (1966, 1978), and Williamson (1988). Generally speaking, the laminar range extends to Re=200, a transitional range from Re=200 to 350, and the high range of Re above 350. Several definitions of the vortex formation region length, or its extent in the streamwise direction, have been proposed over the past forty years:

i) the *minimum* of the mean pressure on the wake axis, or centerline;

ii) the *maximum* of the wake velocity fluctuation at the fundamental shedding or Strouhal frequency, off the wake centerline;

iii) the *maximum* of the wake velocity fluctuation at twice the shedding frequency, on the wake centerline;

iv) the *minimum* cross-stream or lateral spacing, close to the body base region, of the maxima of the velocity fluctuation field.

The first definition of the formation region given here was proposed by Roshko (1954, 1955), based upon measurements of the near-wake pressure and velocity fields for several bluff bodies at high Reynolds numbers (above 350). The third was proposed originally by Gerrard (1966), for the same high Reynolds numbers, and by Griffin (1974), for low Reynolds number wakes. The second and fourth definitions were introduced by Schaefer and Eskinazi (1959) for circular cylinder wakes at low Reynolds numbers, and by Bearman (1965) for blunt-based bluff bodies at high Reynolds numbers.

The recent experiments of Green and Gerrard (1993) and subsequent discussion of these experiments (Griffin, 1995) have shown fairly conclusively that the end of the formation region coincides with the location of maximum vortex strength in the wake of a stationary cylinder. The flow in the vortex formation region plays an important role in the lock-on shedding processes as well.

3 CROSSFLOW OSCILLATIONS

The review papers by Sarpkaya (1979), Bearman (1984), and Griffin and Hall (1991) deal with crossflow oscillations of flexibly-mounted bluff

bodies, bodies which are free to oscillate, and those which are forced to do so. The basic character of the crossflow lock-on boundaries which accompany forced oscillations in the *primary or fundamental* regime as it is called by Williamson and Roshko (1988) can be represented by the measurements of Koopmann (1967) and of Cheng and Moretti (1991) which are plotted in Fig. 1. The former experiments were performed at *Re*=100, 200 and 300 in air, while the latter were performed at *Re*=1500 and 1650 in water. The lock-on boundaries were determined by Cheng and Moretti from a comparison of frequency spectra. Koopmann made his determination from a comparison of osilloscope traces.

Nonetheless there is reasonably good agreement between the two experiments even with the differences in fluid media and Reynolds number. The extent of the lock-on region at oscillation frequencies below the Strouhal frequency, or $f/f_S<1$, is greater than for frequencies above the Strouhal frequency, or $f/f_S>1$, in both experiments. The most surprising feature of the Cheng and Moretti experiments is that the lock-on approaches a well-defined limit at the higher amplitudes. The 'onion shaped' appearance of the boundary is indicative of a form of self-limiting behavior at the upper boundary. Koopmann in his NRL experiments was not able to reach these large amplitudes, nor did one of the authors (O.M.G.) in validating Koopmann's experiments. The maximum extent in amplitude of the lock-on region of y/D~ 0.7 to 0.8 occurs at f/f_S=0.8 to 0.9 and defines the primary lock-on limit.

Some understanding of the crossflow lock-on behavior can be gained from flow visualization of the vortex shedding at *Re*=200. Three visualizations of the vortex street downstream of the oscillating cylinder are shown in Fig. 2, at the frequency condition f/f_S=0.9 and at three amplitudes of y/D=0.25, 0.4 and 0.5, measured from the stationary cylinder's rest position. The visualization was accomplished by injecting a sheet of aerosol particles into the wind tunnel as described by Griffin and Ramberg (1974, 1976). The photographs in this paper have never been published previously. As the amplitude of oscillation is increased the lateral spacing of the vortices decreases until the street becomes almost collinear in Fig. 2(b). At the oscillation amplitude of y/D=0.5 in Fig. 2(c) the first appearance of secondary vortex formation just begins to appear, as the uppermost bound of the lock-on is approached.

When the amplitude of oscillation is increased still further to y/D=0.6 the transition to a new pattern of vortex shedding is completed as the upper boundary is reached and the flow field adjusts to preclude the transition to a thrust-type street of vortices. The result is a more complex pattern of three vortices shed during each cycle of the oscillation as shown in Fig. 3. This transition from the fundamental lock-on to a more complex flow was observed by Williamson and Roshko. They called this a transition from the 2S to the P+S type of vortex pattern. The 2S type is the typical street of alternately signed vortices shed during each oscillation cycle as in Figs. 2(a) and 2(b). The P+S type is the shedding of a vortex pair and a single vortex during each oscillation cycle as shown in Fig. 3.

The shedding pattern at the higher frequency of f/f_S =1.0 and y/D=0.5 is shown in Fig. 4. Once again the street is nearly collinear with very small lateral spacing near the upper lock-on boundary for these oscillations at the Strouhal frequency f_S. The pattern in Fig. 4 undergoes a transition at higher amplitudes of oscillation to a P+S type pattern similar to Fig. 3.

When the oscillation frequency is increased to f/f_S=1.05, the wake adjusts as shown in Fig. 5. Near the upper frequency boundary of the lock-on region the longitudinal spacing of the vortex pattern contracts, as compared to expanding relative to the natural shedding value at the lower frequencies where $f/f_S<1$. The vortex street again appears to be on the verge of transition and instability at the higher amplitude of y/D=0.4. This behavior of the flow is similar to the shedding patterns at high amplitudes near the upper boundary in Figs. 3 and 4.

Another comprehensive experimental study of crossflow oscillations is that of Ongoren and Rockwell. The Reynolds number range of the experiments was *Re* = 580 to 1300. They found that two fundamental types of lock-on take place. At a frequency of one-half of the Strouhal frequency a subharmonic form of lock-on takes place whereby the vortex is always shed from one side of the body, whereas at frequencies near the Strouhal frequency the fundamental form of lock-on takes place as vortices are shed alternately from the body to form the altered Karman vortex street pattern.

The formation region of the vortices varies inversely in length with frequency in the lock-on regime (Griffin and Ramberg 1974; Ongoren and Rockwell 1988), and is reduced in length by increasing the amplitude of oscillation at any given constant frequency as well. These changes in the vortex formation are accompanied by corresponding adjustments in the strength or circulation of the vortices.

Zdravkovich (1982) found from studying numerous flow visualization experiments existing at the time that a rapid transition in the phase of the vortex shedding, relative to the body oscillations, takes place in the vicinity of the natural shedding frequency. This phase shift results in a switch in the shedding of the initially shed vortex from the upper to the lower side of the cylinder or vice versa. For $f/f_s > 1$ the vortex forms on one side of the cylinder and forms when the cylinder reaches the peak amplitude on the opposite side. For frequencies in the range $f/f_s < 1$ the timing of the shedding changes abruptly and the vortex sheds at the peak amplitude on the same side as the forming vortex. The phase shift also governs that portion of the lock-on regime where energy is transferred from the flow to the cylinder (self-excited oscillations are possible). The phase shift and energy transfer in the fundamental lock-on regime recently has been studied further by Gopalkrishnan, Grosenbaugh and Triantafyllou (1992).

The boundaries of this lock-on regime have been computed by Meneghini and Bearman (1993). The vortex shedding was computed in two dimensions using a hybrid vortex-in-cell method which incorporates viscous diffusion as well. The upper and lower bounds of the lock-on and nonlock-on states are plotted here in Fig. 5 which is adapted from Meneghini and Bearman. The lower y/D boundary changes with oscillation frequency and compares very well with Koopmann's wind tunnel experiments in Fig. 1 at amplitudes below y/D~0.5. The primary lock-on boundaries measured in water by Cheng and Moretti extend to somewhat lower oscillation frequencies. The computed upper boundary is essentially a straight line near y/D=0.65 and does not exhibit the 'onion shaped' variation with amplitude that was measured by Cheng and Moretti. The reasons for this lack of agreement between the computations and the experiments near the upper boundary is not clear, but may be due to the differences in Reynolds number, differences in media (water vs. air), and limitations imposed by the two-dimensional computations. This is an unresolved question at the present time.

Several computed wake patterns are shown here in Figs. 7 and 8 where the shedding is visualized numerically by a 'cloud' of point vortices. In the computations the cylinder always is at its uppermost position when the visualization is recorded. It is remarkable to observe the similarities between the computed flows at $Re = 200$ and the flow visualization of the wake pattern at the same Re in Figs. 2 to 5. The changes in length of the vortex formation region with frequency of oscillation are evident in the computed flow fields as well as in the experimental visualizations.

The contraction of the longitudinal spacing with increasing oscillation frequency at lock-on is clear from the patterns in Fig. 7. The transition from the fundamental lock-on pattern where a pair of vortices is shed during each cycle of the oscillation to the complex pattern of three vortices at the higher amplitudes of oscillation is shown computationally in Fig. 8. The corresponding experimental visualization of this transition is shown in Figs. 2 and 3. Both the experiments and the computations provide a faithful representation of numerous features of the real flow geometry even though the computations are limited to two dimensions.

4 FLOW PERTURBATIONS AND IN-LINE OSCILLATIONS

The experiments of Barbi, et al. (1986) were performed to examine the vortex lock-on for a cylinder in a steady uniform flow with a superimposed periodic velocity component. The results show some very basic similarities with the earlier in-line oscillation experiments of Griffin and Ramberg (1976). The vortex lock-on measurements by Barbi, et al. are compared with those of Griffin and Ramberg in Fig. 9. The vertical axis represents two different measures of the perturbation amplitude. For the experiments of Griffin and Ramberg the peak-to-peak amplitude of cylinder displacement is given by 2x/D. And for the experiments of Barbi et al. the peak-to-peak incident velocity perturbation is given by $2\Delta u/\omega D$. The horizontal axis is again the ratio of the vibration frequency f and the Strouhal frequency f_s of a stationary cylinder. The two types of external disturbance are equivalent for the conditions shown in the figure.

Also shown are the circular cylinder oscillation results of Tanida, Okajima and Watanabe (1973) and of Tatsuno (1972), reproduced from the paper by Griffin and Ramberg. Vortex lock-on and crossflow oscillations usually occur near the Strouhal shedding frequency f_s. For in-line oscillations and flow perturbations the lock-on is found at frequencies near twice the Strouhal frequency, $2f_s$, since the the forcing fluctuations in the drag force are in the flow direction. However, in many cases the actual lock-on frequency extends to near the Strouhal frequency, which is nominally half the oscillation or perturbation frequency.

There is generally good agreement between the bounds of the lock-on regime for the two different types of external disturbance or flow control, though there is some scatter at the highest perturbation amplitudes. This is most likely due to Reynolds number effects, as noted by Barbi et al. The latter experiments were conducted at *Re* between 3,000 and 40,000, whereas the results of Tanida, et al., Tatsuno, and of Griffin and Ramberg were conducted at *Re* between 80 and 4,000. The overall agreement is quite good.

The base pressure is reduced (becomes more negative) and the mean drag coefficient C_D is increased in a corresponding way for the perturbed flow as compared to the unperturbed flow (Griffin and Hall 1991). These changes in the near-wake force and pressure fields are analogous to those observed for the crossflow oscillations.

Recent advances in computational fluid dynamics such as those of Karniadakis and Triantafyllou (1989, 1992) and of Meneghini and Bearman (1993) permit new insights into the effects of cylinder oscillations on the bluff body near-wake. The computations by Hall and Griffin (1993), which are summarized briefly here, allow the superposition of an oscillatory component on the inflow boundary condition for a domain such as the spectral element grid. The ensuing lock-on for this flow was studied by direct numerical simulation of the two-dimensional flow past a circular cylinder at *Re*= 200. The computations employed a variation of the spectral element formulation developed by Karniadakis and Triantafyllou.

A perturbed boundary condition of the form

$$U_x = 1.0 + \Delta u \sin \omega t,\ U_y = 0.$$

was enforced at the inflow, where U_x and U_y denote the x- and y-components of the velocity, respectively. Here $\Delta u = a\,\omega$, where $\omega = 2\,\pi\,f$, and the perturbation frequency $f = 2\,\alpha\,f_s$. The parameter a varied from 0.05 to 0.25, while α varied to give perturbation frequencies ranging from $1.4\,f_s$ to $2.8\,f_s$ (see Fig.10). Each closed circle or cross in this figure represents a direct numerical simulation by Hall and Griffin. The primary or fundamental lock-on are indicated by the closed circles.

The shaded regions in Fig. 10 represent boundaries across which breakdown occurs, or receptivity boundaries as they are described by Karniadakis and Triantafyllou (1989), from a periodic, locked-on flow to a non-periodic or quasi-periodic or chaotic flow in which the primary frequency is the natural shedding frequency rather than the perturbation. The width of this region is not defined precisely, but only bracketed here. In all of the cases lying outside of the lock-on region, the flow continues to be strongly influenced by the perturbation, as shown by the chaotic nature of the flow in contrast with the regular, periodic natural shedding. Nonlock-on is defined as the condition for which the highest peak in the spectrum occurs at the natural shedding frequency or at a frequency corresponding to neither the perturbation nor the natural shedding frequency (Hall and Griffin, 1993).

Several cases in Fig. 11 are examined. For cases *a*, *b*, *d* and *e* the amplitude of the perturbation is held fixed while the frequency is increased from 1.5 f_s(case *a*) to 2.4 f_s (case *e*). A forcing frequency of 1.5 f_s results in a nonperiodic velocity history with the spectrum in Fig. 11(a), which shows clearly the chaotic nature of the flow. The highest peak in the spectrum occurs just below the natural shedding frequency of $St = 0.195$. Increasing the forcing frequency from 1.5 f_s to 1.6 f_s results in case *b* in Fig. 10. The flow is periodic, with shedding frequency equal to 0.8 f_s, and thus lock-on has occurred. The flow pattern is more complex than that of the unperturbed case, and the spectrum in Fig. 11(b) shows that there is now more energy in the higher harmonics of the perturbation frequency than in higher harmonics of f_s.

Moving to the right in Fig.11, we again increase the perturbation frequency to 2.3 f_s for case *d*. Lock-on again takes place, this time at a frequency of 1.15 f_s. The spectrum corresponding to this case is shown in Fig. 11(c). The results from case *e* demonstrate that the shaded region has been crossed and that the flow again is outside of the lock-on region. The dominant peak in the spectrum in Fig. 11(d) occurs at neither the natural shedding frequency nor the perturbation frequency. The three highest peaks in the spectrum are labeled. Peak number one occurs just above the natural shedding frequency at approximately $St = 0.2$, peak number two occurs at half the perturbation frequency or $St = 0.23$, and peak number three occurs at the sum of these, or $St = 0.43$. Thus peak three, the highest, is a higher harmonic of neither the natural shedding frequency nor the perturbation frequency, but of the average of the two. This is indicative of an intermittent and transitional region near the lock-on boundary. A more extensive discussion of the spectral character of the flow at and near the lock-on conditions represented in Fig. 10 is given by Hall and Griffin (1993).

As an example of the near-wake flow at lock-on, we briefly examine case *g*. Time averaging was done